Statistical Fluctuations of Energy Spectrum, Electromagnetic Transitions and Electromagnetic Moments in ^{136}Xe Nucleus Using the Framework of Nuclear Shell Model

A. K. Hamoudi

Department of Physics, College of Science, University of Baghdad, Baghdad, Iraq
E-mail: a.hamoudi@yahoo.com

Abstract

The fluctuation properties of energy spectrum, electromagnetic transition intensities and electromagnetic moments in ^{136}Xe nucleus are investigated with realistic shell model calculations. We find that the spectral fluctuations of ^{136}Xe are consistent with the Gaussian orthogonal ensemble of random matrices. Besides, we observe a transition from an order to chaos when the excitation energy is increased and a clear quantum signature of the breaking of chaoticity when the single-particle energies are increased. The distributions of the transition intensities and of the electromagnetic moments are well described by a Porter-Thomas distribution. The statistics of electromagnetic transition intensities clearly deviate from a Porter-Thomas distribution (i.e., a transition towards regularity is observed) when the single-particle energies are increased whereas the statistics of electromagnetic moments are not affected by the change of the single-particle energies.

Keywords
Chaos in nuclei, Shell model calculations

Article info
Received: Mar. 2010
Accepted: Apr. 2010
Published: Oct. 2010

التموجات الأحصائية للطيف الطاقي ولشدة الأنتقالات والعزوم الكهرومغناطيسية لنواة ^{136}Xe بأستخدام أنموذج القشرة النووية

عادل خلف حمودي

قسم الفيزياء – كلية العلوم – جامعة بغداد — بغداد – العراق

الخلاصة

أستخدمنا حسابات أنموذج القشرة الواقعية في دراسة الخواص التموجية للطيف الطاقي ولشدة الأنتقالات والعزوم الكهرومغناطيسية في نواة ^{136}Xe. اوضحت هذه الدراسة بأن هذه النواة لها بصمة السلوك الفوضوى نتيجة توافق التموجات الأحصائية الطيفية (المحسوبة ضمن طاقات التهيج العالية) مع النظرية العشوائية للمصفوفات. لقد لاحظنا اعتماد التموجات الأحصائية الطيفية على طاقة التهيج حيث يمكن الأنتقال من بصمة السلوك المنتظم الى السلوك الفوضوى عن طريق زيادة طاقة التهيج للنواة، ولاحظنا أيضا بأن هنالك بصمة واضحة في النتائج تشير الى انهيار (تكسر) السلوك الفوضوي للنواة مع زيادة قيم طاقات الجسيمات المنفردة. اوضحت هذه الدراسة أيضا بأن التموجات الأحصائية لتوزيعات شدة الأنتقالات الكهرومغناطيسية والعزوم الكهرومغناطيسية في نواة ^{136}Xe تتفق تماما مع توزيع بورتر– ثوماس، وهذا دليل اخر يدعم صفة السلوك الفوضوى لهذه النواة. لقد لاحظنا بأن زيادة قيم طاقات الجسيمات المنفردة في الحسابات يسبب أنحراف واضح بين توزيعات شدة الأنتقالات الكهرومغناطيسية وتوزيع بورتر– ثوماس بينما توزيعات العزوم الكهرومغناطيسية تبقى كما هي لاتتأثر بتغير قيم طاقات الجسيمات المنفردة.

Introduction

Quantum chaos has been studied intensely during the last three decades [1]. Bohigas et al. [2] proposed a connection between chaos in a classical system and the spectral fluctuations of the analogous quantum system, where an analytical proof of the Bohigas et al. conjecture has been presented in [3]. It is now generally accepted that quantum analogs of most classically chaotic systems show spectral fluctuations that agree with the random matrix theory (RMT) [4,5] while quantum analogs of classically regular systems show spectral fluctuations that agree with a Poisson distribution. For time-reversal-invariant systems, the appropriate form of RMT is the Gaussian orthogonal ensemble (GOE). RMT was originally employed to describe the statistical fluctuations of neutron resonances in compound nuclei [6]. It has become a standard tool for analyzing the universal statistical fluctuations in chaotic systems [7-10].

The chaotic nature of the single particle dynamics in the nucleus can be studied in terms of the mean field approximation. However, the nuclear residual interaction mixes different mean field configurations and affects the statistical fluctuations of the many particle spectrum and wave functions. These fluctuations can be studied via various nuclear structure models. The statistics of the low-lying collective part of the nuclear spectrum have been studied in the framework of the interacting boson model [11,12], in which the nuclear fermionic space is mapped onto a much smaller space of bosonic degrees of freedom. Because of the relatively small number of degrees of freedom in this model, it was also possible to relate the statistics to the underlying mean field collective dynamics. At higher excitations, additional degrees of freedom (such as broken pairs) become important [13], and the effects of interactions on the statistics must be studied in larger model spaces. The interacting shell model offers an attractive framework for such studies. In this model, realistic effective interactions are available and the basis states are labeled by exact quantum numbers of angular momentum (J), isospin (T) and parity (π) [14].

In the studies [15-19], the distribution of eigenvector components was examined using the framework of the shell model. Brown and Bertsch [17] found that the basis vector amplitudes are consistent with Gaussian distribution (which is the GOE prediction) in regions of high level density but deviated from Gaussian behavior in other regions unless the calculation employs degenerate single particle energies. Later studies [19] also suggested that calculations with degenerate single particle energies are chaotic at lower energies than more realistic calculations. The electromagnetic transition intensities in a nucleus are observables that are sensitive to the wave functions, and the study of their statistical distributions should complement [12,13] the more common spectral analysis and serve as another signature of chaos in quantum systems.

Most studies of statistical properties in the shell model were restricted to lighter nuclei $A \leq 40$ (e.g. *sd*-shell nuclei). In the previous work [20], we carried out the *fp*-shell model calculations for $A = 60$ nuclei (with ^{56}Ni as a core and the remaining valence particles move within $0f_{5/2}$, $1p_{3/2}$ and $1p_{1/2}$ orbitals) and studied the statistical fluctuations of electromagnetic transition intensities and electromagnetic moments using the $F5P$ [21] interaction. The calculated results [20] were in agreement with RMT and with the previous finding of a Gaussian distribution for the eigenvector components [15-19].

There has been no detailed study of the statistical fluctuations in the $N82-$model

space. In this study, we perform shell model calculations for ^{136}Xe (with ^{132}Sn as a core and the remaining four protons move in the $N82$-model space) and investigate the fluctuation properties of energy spectrum, electromagnetic transition intensities and electromagnetic moments. The wave functions are obtained by constructing all possible configurations within the $N82$-model space defined by $2d_{5/2}, 1g_{7/2}, 1h_{11/2}, 3s_{1/2}$ and $2d_{3/2}$ orbitals and diagonalizing the effective interaction of $N82K$ [22] using the shell model program OXBASH [23]. We find that the spectral fluctuations are consistent with the GOE limit and the statistics of both the transition intensities and the electromagnetic moments, obtained using normal single-particle energies, are well described by RMT.

Theory

The fluctuation properties of the nuclear shell model spectrum are determined by means of two statistical measures: the nearest-neighbors level spacing distribution $P(s)$ and the Dyson-Mehta or Δ_3 statistics [4,24]. We first construct the staircase function of the nuclear shell model spectrum $N(E)$, defined as the number of levels with excitation energies less than or equal to E. The level spectrum is then mapped onto unfolded levels using the method of Ref [12]

$$\tilde{E}_i = N(E_i) \qquad (1)$$

The unfolded levels $\tilde{E}_i$ have a constant average spacing, but the actual spacings show strong fluctuations.

The level spacing distribution (which characterizes the fluctuations of the short-range correlations between energy levels) is defined as the probability of two neighboring levels to be a distance s apart. A regular system is expected to behave by the Poisson statistics

$$P(s) = \exp(-s) \qquad (2)$$

If the system is classically chaotic, we expect to obtain the Wigner distribution

$$P(s) = (\pi/2)s\exp(-\pi s^2/4) \qquad (3)$$

which is consistent with the GOE statistics.

To quantify the chaoticity of $P(s)$ by means of a parameter, we compare it to the Brody distribution

$$P(s,\omega) = \alpha(\omega+1)s^{\omega}\exp(-\alpha s^{\omega+1}) \qquad (4)$$

where

$$\alpha = \left(\Gamma\left[\frac{\omega+2}{\omega+1}\right]\right)^{\omega+1} \qquad (5)$$

This distribution interpolates between the Poisson distribution $(\omega = 0)$ of regular systems and the Wigner distribution $(\omega = 1)$ of chaotic systems (GOE). The parameter ω can be used as a simple quantitative measure of the degree of chaoticity [25].

The Δ_3 statistic (which describes the fluctuations of the long-range correlations between energy levels) is used to measure the rigidity of the nuclear spectrum and defined by [4]

$$\Delta_3(\alpha, L) = \min_{A,B}\frac{1}{L} \times \int_{\alpha}^{\alpha+L}\left[N(\tilde{E}) - (A\tilde{E}+B)\right]^2 d\tilde{E} \qquad (6)$$

It measures the deviation of the staircase function (of the unfolded spectrum) from a straight line. A rigid spectrum corresponds to smaller values of Δ_3 whereas a soft spectrum has a larger Δ_3. In the Poisson limit, $\Delta_3(L) = L/15$. In the GOE limit, $\Delta_3 \approx L/15$ for small L, while $\Delta_3 \approx \pi^{-2}\ln L$ for large L.

The fluctuation properties of electromagnetic transition rates are also considered. Since the matrix elements of electromagnetic transition operators probe system's wave functions so that their statistical fluctuations provide additional information. The electromagnetic transition

probability from an initial state $|i\rangle$ to a final state $|f\rangle$ is given by [26]

$$B(\varpi L; J_i T_i T_z \rightarrow J_f T_f T_z) = \frac{\left|\delta_{T_i T_f} M_{is}(\varpi L) - < T_i T_z 10 | T_f T_z > M_{iv}(\varpi L)\right|^2}{(2J_i + 1)(2T_i + 1)} \quad (7)$$

where ϖ represents the electric (E) or magnetic (M) character of the transition and 2^L represents the multipolarity. The quantities $M_{is}(\varpi L)$ and $M_{iv}(\varpi L)$ are the triply reduced matrix elements for the isoscalar and isovector components of the transition operator, respectively. It should be noted that these matrix elements depend on J_i, T_i and J_f, T_f but not on T_z. For $\Delta T = 0$ transitions (i.e., $T_i = T_f = T$), the isospin Clebsch-Gordon coefficient in eq. (7) is simply given by

$$< TT_z 10 | TT_z > = T_z / \sqrt{T(T+1)} \quad (8)$$

Results and discussion

To examine the validity of RMT in the above model space, we first analyze the energy level fluctuations for states (which have the same parity) with good spin and isospin. We have calculated the spacings s_i from the unfolded levels by $s_i = \tilde{E}_{i+1} - \tilde{E}_i$. To obtain a reliable statistical analysis, we need to consider a sufficiently large number of level spacings. To do so we combine the level spacings of different J in a nucleus to calculate the $P(s)$ distribution. Here, we include all level spacings for $0^+ \le J^\pi \le 9^+$ states in ^{136}Xe nucleus.

Figure 1 displays the calculated $P(s)$ distribution (histograms) for the $0^+ \le J^\pi \le 9^+$ set of level spacings in ^{136}Xe nucleus up to a fixed value of the excitation energy $E = 4$ MeV [Fig. 1(a)], 8 MeV [Fig. 1(b)] and 12 MeV [Fig. 1(c)]. The number of spacings up to 4, 8 and 12 MeV is 45, 407 and 1127 respectively. To study the energy dependence of the chaoticity in ^{136}Xe, we display the best fit Brody distribution (solid line) as well as its parameter ω. It is noticed that the Brody parameter ω increases with the excitation energy, i.e. states at higher energy are much chaotic than those at lower energy. Thus, the level repulsion at small spacings (which is a distinctive feature of chaotic level statistics) increases with the excitation energy. It is evident that the calculated histograms up to 4 and 8 MeV [Figs. 1(a) and 1(b), respectively] are not fully chaotic while the one calculated up to 12 MeV [Fig. 1(c)] is in accordance with the Wigner distribution (dashed line). The Poisson distribution (dash-dotted line), which corresponds to a random sequence of levels and describes regular systems, is also shown for comparison.

Another important aspect is the effect of the one body Hamiltonian on the $P(s)$ distribution. The single-particle motion in the spherical mean field is regular, while the nuclear two-body residual interaction is strongly nonlinear. Fig. 2 illustrates how the energy level fluctuations in ^{136}Xe change when single-particle energies are changed. The top and bottom panels correspond to the calculated $P(s)$ (histograms), for $0^+ \le J \le 9^+$ states in the ^{136}Xe, obtained using the normal and double value of experimental single-particle energies (for $2d_{5/2}, 1g_{7/2}, 1h_{11/2}, 3s_{1/2}$ and $2d_{3/2}$ orbitals), respectively. The realistic residual interaction is the same in both panels. The histograms are calculated up to excitation energy 6 MeV [Figs. 2(a) and 2(c)] and for the whole energy spectrum [Figs. 2(b) and 2(d)]. The dashed, dash-dotted and solid lines stand for GOE, Poisson and Brody distributions, respectively. For the normal

value of single-particle energies, the calculated histograms [Figs. 2(a) and 2(b)] demonstrate chaotic dynamics, where the Brody parameters are $\omega = 0.85$ and 0.99 respectively. Increasing the value of single-particle energies by a factor of 2 leads to a transition towards regularity as seen in the calculated histograms of Figs. 2(c) and 2(d), where the Brody parameters are now reduced to $\omega = 0.30$ and 0.49, respectively.

For considering the fluctuations of the spectral rigidity we calculate the Δ_3 statistics for a set of levels with fixed J and then compute the average Δ_3 of several J values, in order to improve the statistics. Figure 3 demonstrates the Δ_3 dependence on the single-particle energies. The average Δ_3 for all $0^+ \le J^\pi \le 9^+$ states in ^{136}Xe (where the whole energy spectrum is considered) is plotted using the normal and double value of single-particle energies. It is obviously observed that for normal value of single-particle energies, the calculated Δ_3 (filled circles) agrees well with the GOE limit (the solid line) and for double value of single-particle energies, the calculated Δ_3 (open squares) becomes closer to the Poisson limit (the dashed line). It is evident from this figure that the chaoticity in ^{136}Xe nucleus, measured in terms of Δ_3 statistics, is strongly dependent on the single-particle energies. This behavior confirms the results that we obtained from the analysis of the $P(s)$ distribution.

To analyze the fluctuation properties of electromagnetic transition rates, it is necessary to divide out any secular variation of the average strength function versus the initial and final energies. We do this by applying the method of Ref. [12]. The average transition strength at an initial energy E and final energy E' is calculated from:

$$< B(\overline{\omega}L; E, E') > = \frac{\sum_{i,f} B(\overline{\omega}L; i \to f) e^{-(E-E_i)^2/2\gamma^2} e^{-(E'-E_f)^2/2\gamma^2}}{\sum_{i,f} e^{-(E-E_i)^2/2\gamma^2} e^{-(E'-E_f)^2/2\gamma^2}} \quad (9)$$

where γ is a parameter chosen as described below. For fixed values of the initial (J_i, T) and final (J_f, T) states, we calculate from eq. (7) the intensities $B(\overline{\omega}L; i \to f)$. All transitions of a given operator (e.g., $M1$ or $E2$) between the initial and final states of the given spin and isospin classes have been included in the statistics. The energy levels used in eq. (9) are the unfolded energy levels characterized by a constant mean spacing. The value of γ in eq. (9) has been chosen to be large enough to minimize effects arising from the local fluctuations in the transition strength but not so large as to wash away the secular energy variation of the average intensity. In this study we use $\gamma = 2.5$. We renormalize the actual intensities by dividing out their smooth part

$$y_{fi} = \frac{B(\overline{\omega}L; J_i T T_z \to J_f T T_z)}{< B(\overline{\omega}L; E, E') >} \quad (10)$$

and construct their distribution using bins that are equally spaced in $\log_{10} y$. The choice of $\log_{10} y$ as the variable allows us to display the distribution of the weak transitions over several orders of magnitude. In RMT we expect a Porter-Thomas distribution for $P(y)$, i.e., a χ^2 distribution in $\nu = 1$ degrees of freedom [20]. A χ^2 distribution in ν degrees of freedom is given by

$$P_\nu(y) = (\nu / 2 < y >)^{\nu/2} \times y^{\nu/2-1} e^{-\nu y/2<y>} / \Gamma(\nu/2) \quad (11)$$

In RMT, the matrix element $\langle f | \hat{T} | i \rangle$ of the transition operator $\hat{T}$ between an initial state $\langle i |$ and a final state $| f \rangle$ is a Gaussian

variable with a zero average, i.e. $\overline{\langle f|\hat{T}|i\rangle} = 0$, [20]. The transition intensity is proportional to the square of the matrix element $\langle f|\hat{T}|i\rangle$ and thus has a Porter-Thomas distribution [i.e., eq. (11) with $\nu = 1$].

We have tested the distribution of $B(E2)$ and $B(M1)$ $2^+ \rightarrow 2^+$ transitions in the ^{136}Xe nucleus. For each transition operator we have sampled $166^2 - 166 = 27390$ transition matrix elements. Fig. 4 shows the calculated distributions (histograms) of the $B(E2)$ [Figs. 4(a) and 4(c)] and $B(M1)$ [Figs. 4(b) and 4(d)] $2^+ \rightarrow 2^+$ transitions. The top and bottom panels correspond to the normal and double value of single-particle energies, respectively. It is clear from the top panel that the calculated histograms of $B(E2)$ [Fig. 4(a)] and $B(M1)$ [Fig. 4(b)] are well described by a Porter-Thomas distribution (solid line), but those of bottom panel [Figs. 4(c) and 4(d)] clearly deviate from the Porter-Thomas distribution. This deviation indicates that there is a transition towards regularity due to the increase of the value of single-particle energies, where this behavior is in agreement with the trend previously obtained from the analysis of both the $P(s)$ and Δ_3 statistics.

In the case of quantum numbers of the initial and final states are identical, we can also examine the statistics of the diagonal matrix elements $\langle i|\hat{T}|i\rangle$. However, we still here find that $\langle i|\hat{T}|i\rangle$ is a Gaussian variable but with a nonzero average,

$$\overline{\langle i|\hat{T}|i\rangle} = \frac{1}{N_i} Tr(P_i \hat{T}) \qquad (12)$$

where P_i is the projection operator on the N_i-dimensional subspace of eigenstates with quantum numbers J_i^{π}, T_i. Because the average value of diagonal matrix elements is nonzero, the square of $\langle i|\hat{T}|i\rangle$ does not follow a Porter-Thomas distribution. However, once the average value of eq. (12) has been subtracted from the diagonal matrix elements, their squares z are predicted to have a Porter-Thomas distribution. Fig. 5 illustrates the distributions of the squares of these shifted reduced diagonal matrix elements (using the normal single-particle energies) for the $E2$ electric quadrupole moments [Fig. 5(a)] and $M1$ magnetic dipole moments [Fig. 5(b)] of $J^{\pi} = 2^+$ states in the ^{136}Xe nucleus. The values of z are renormalized by dividing out the secular variation with energy of the square of the reduced diagonal matrix element, defined by an equation similar to eq. (9) but with a single Gaussian (since $i = f$). Considering the small number of data points used to compute the distribution $P(\log_{10} z)$ (there are only 166 diagonal matrix elements), the agreement with a Porter-Thomas distribution (solid lines) is reasonable. Similar results have been found, as in Fig. 5, for the double value of single-particle energies. It is found that the statistics of $E2$ and $M1$ moments of the $J^{\pi} = 2^+$ states are not affected by the change of the single-particle energies.

Conclusions

The statistical fluctuations of energy spectrum, electromagnetic transition intensities and electromagnetic moments in ^{136}Xe nucleus were analyzed using the shell model calculations with the realistic interaction of $N82K$. It is found that the spectral fluctuations of ^{136}Xe are in consistent with the GOE limit. Besides, a transition from an order to chaos is seen when the excitation energy is increased and a clear quantum signature of the breaking of chaoticity is also seen when the single-particle energies are increased. The statistics of $B(E2)$ and $B(M1)$ transitions and of $E2$

and $M1$ moments show chaotic dynamics in ^{136}Xe (i.e., they follow a Porter-Thomas distribution). The statistics of electromagnetic transition intensities deviate from a Porter-Thomas distribution (i.e., a transition towards regularity is observed) when the single-particle energies are increased, whereas the statistics of electromagnetic moments are not affected by the change of the single-particle energies.

References

[1] F. Haak: *Quantum signature of chaos* (Springer-Verlag, Berlin, **(2001)** 2nd enlarged ed.

[2] O. Bohigas, M. J. Giannoni and C. *Schmit*: Phys. Rev. Lett. 52 **(1986)** 1.

[3] S. Heusler, S. Muller, A. Altland, P. *Braun, and F. Haak: Phys. Rev. Lett.* 98 **(2007)** 044103.

[4] M. L. Mehta: *Random Matrices* (*Academic* Press, New York, **(2004)** 3nd ed..

[5] T. Papenbrock, and H. A. *Weidenmuller*: Rev. Mod. Phys., Vol. 79, No. 3 **(2007)** 997

[6] C. E. Porter: *Statistical Theories of Spectra: Fluctuations* (Academic Press, New York **(1965)**.

[7] T. A. Brody, J. Flores, J. B. French, P. A. Mello, A. Pandey and S. S. M. Wong: Rev. Mod. Phys. 53 **(1981)** 385.

[8] T. Guhr, A. M*ü* ller-Groeling and H. A. *Weidenm*ü ller: Phys. Rep. 299, **(1998)** 189.

[9] Y. Alhassid: Rev. Mod. Phys. 72 **(2000)** 895.

[10] M. C. Gutzwiller: *Chaos in Classical and Quantum Mechanics* (Springer-Verlag, New York, **(1990)**.

[11] Y. Alhassid, A. Novoselsky and N. Whelan: Phys. Rev. Lett. 65 **(1990)** 2971; Y. Alhassid and N. Whelan: Phys. Rev. C 43 **(1991)** 2637.

[12] Y. Alhassid and A. Novoselsky: Phys. *Rev*. C 45 **(1992)** 1677.

[13] Y. Alhassid and D. Vretenar: Phys. Rev. C 46 **(1992)** 1334.

[14] V. Zelevinsky, B. A. Brown, N. frazier and M. Horoi: Phys. Rep. 276 **(1996)** 87.

[15] R. R. Whitehead et al: Phys. Lett. B 76 **(1978)** 149.

[16] J. J. M. Verbaarschot and P. J. *Brussaard*: Phys. Lett. B 87 **(1979)** 155.

[17] B. A. Brown and G. Bertsch: Phys. Lett. B 148 **(1984)** 5.

[18] H. Dias et al.: J. Phys. G 15 **(1989)** *L79.*

[19] V. Zelevinsky, M. Horoi and B. A. Brown: Phys. Lett. B 350 **(1995)** 141.

[20] A. Hamoudi, R. G. Nazmidinov, E. *Shhaliev* and Y. Alhassid: Phys. Rev. C65 **(2002)** 064311.

[21] P. W. M. Glaudemans, P. J. *Brussaard* and R. H. Wildenthal: Nucl. Phys. A 102 **(1976)** 593.

[22] H. G. Kruse and B. H. Wildenthal: Bull. An. Phys. Soc. 27 **(1982)** 533.

[23] A. B. Brown, A. Etchegoyen, N. S. Godin, W. D. M. Rae, W. A. Richter, W. E. Ormand, E. K. Warburton, J. S. Winfield, L. Zhao and C. H. Zimmermam: *MSU-NSCL Report Number 1289.*

[24] F. S. Stephens, M. A. Deleplanque, I.Y. Lee, A. O. Macchiavelli, D. Ward, P. Fallon, M. Cromaz, R. M. Clark, M. Descovich, R. M. Diamond, and E. Rodriguez-Vieitez: Phys. Rev. Lett., 94 **(2005)** 042501.

[25] J. M. G. Gomez, V. R. Manfredi, L. *Salasnich*, and E. Gaurier: Phys. Rev. C58, No.4 (1998) 2108.

[26] P. J. Brussaard and P. W. M. *Glaudemans*: *Shell-Model Applications in Nuclear Spectroscopy* (North-Holland, Amsterdam **(1977)**.

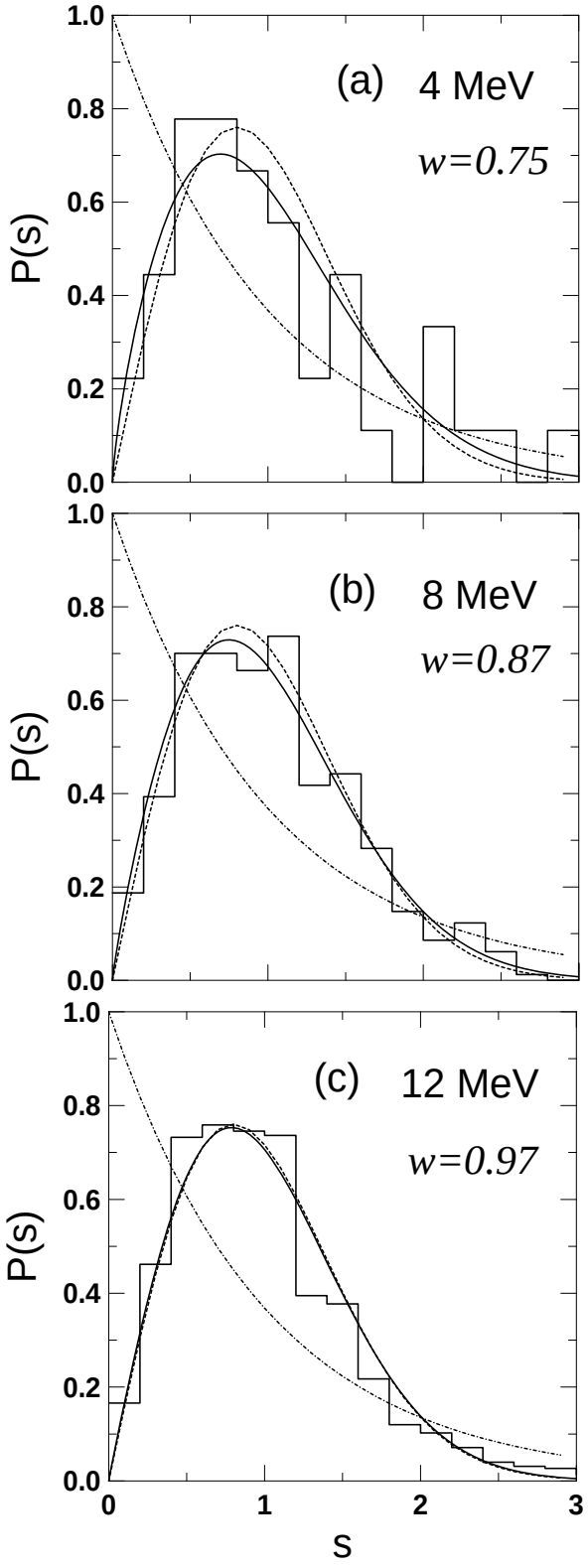

Fig.1. The $P(s)$ ***distribution for*** $0^+ \le J \le 9^+$ ***states in the*** ^{136}Xe***. The histograms are calculated up to excitation energy (a) 4 MeV, (b) 8 MeV and (c) 12 MeV. The dashed, dash-dotted and solid lines stand for GOE, Poisson and Brody distributions, respectively.***

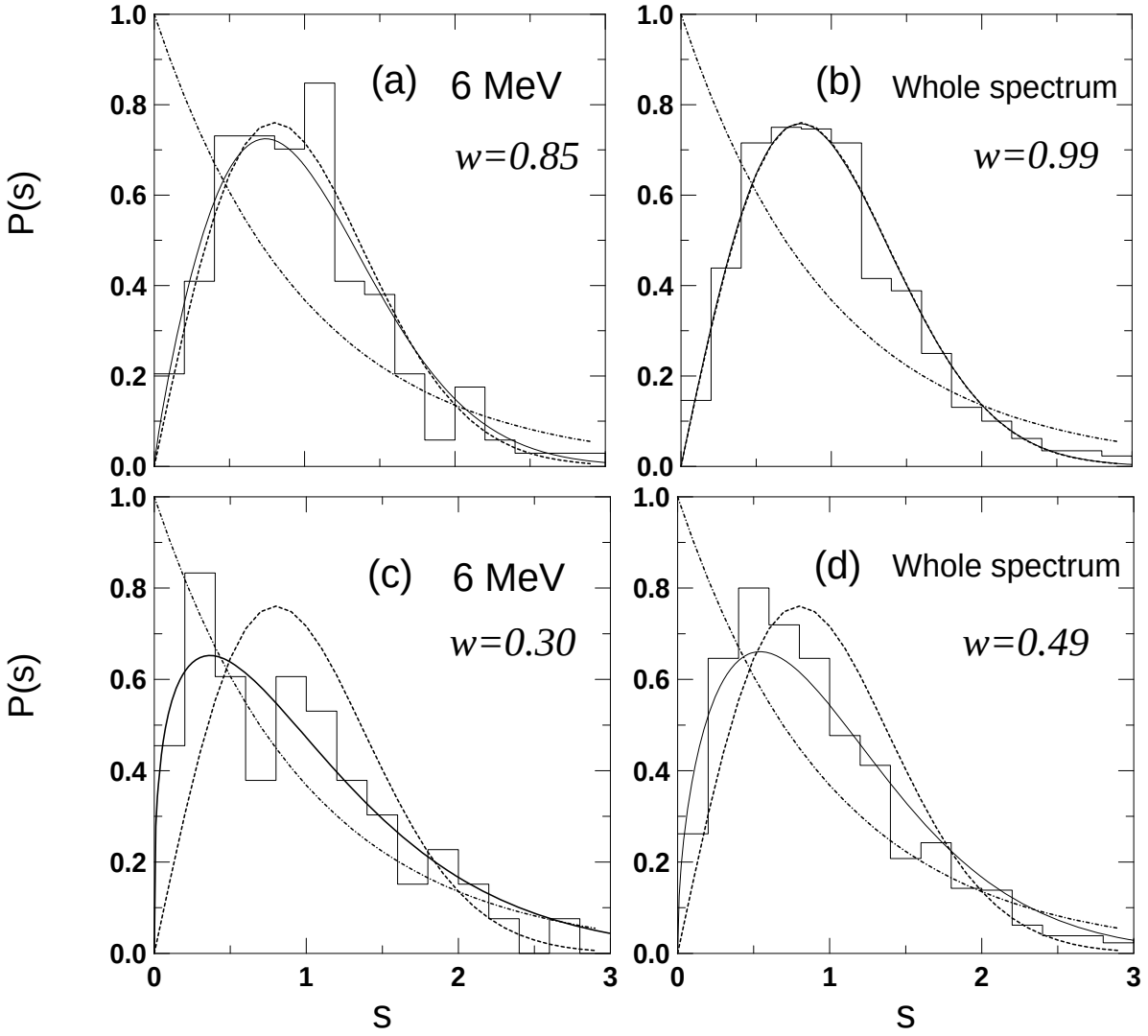

Fig.2. The $P(s)$ ***distribution for*** $0^+ \le J \le 9^+$ ***states in the*** ^{136}Xe***. The top and bottom panels correspond to the calculated distribution (histograms) obtained using normal and double value of single-particle energies, respectively. The histograms are calculated up to an excitation energy 6 MeV [(a) and (c)] and for the whole energy spectrum [(b) and (d)]. The dashed, dash-dotted and solid lines stand for GOE, Poisson and Brody distributions, respectively.***

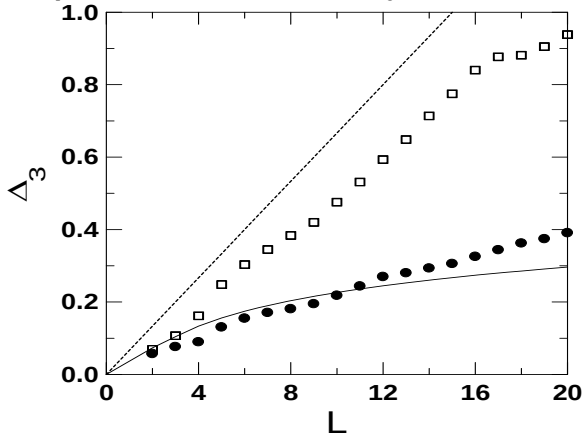

Fig.3. Average Δ_3 ***for all*** $0^+ \le J^\pi \le 9^+$ ***states in*** ^{136}Xe ***(the whole energy spectrum is considered) is calculated using the normal value of single-particle energies (filled circles) and double value of single-particle energies (open squares). The solid and dashed lines stand for GOE and Poisson limits, respectively.***

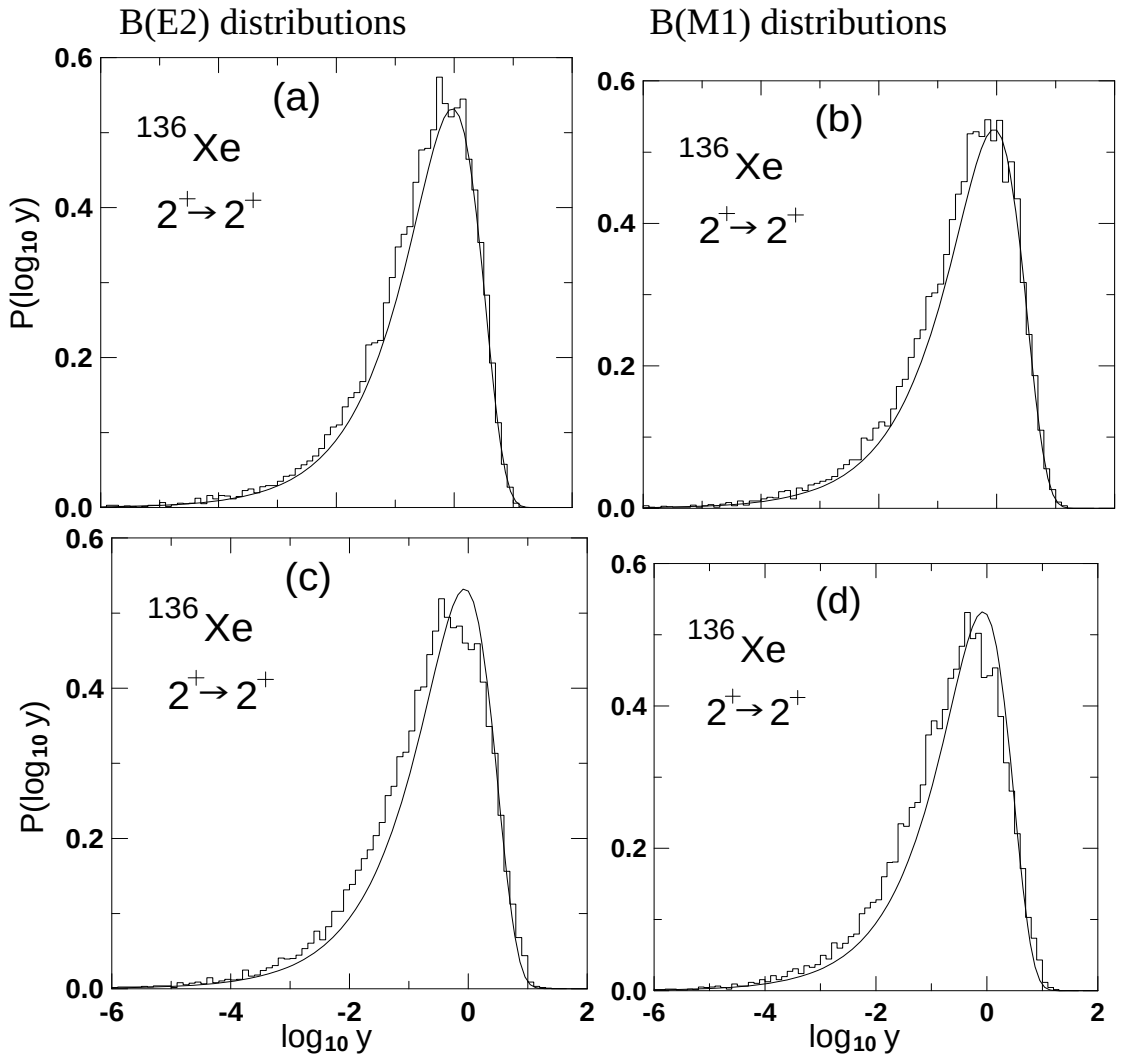

Fig.4. The calculated $B(E2)$ ***[(a) and (c)] and*** $B(M1)$ ***[(b) and (d)] intensity distributions (histograms) for the*** $2^+ \rightarrow 2^+$ ***transitions in*** ^{136}Xe ***nucleus. The top and bottom panels correspond to the normal and double value of single-particle energies, respectively. The solid lines describe Porter-Thomas distribution***.

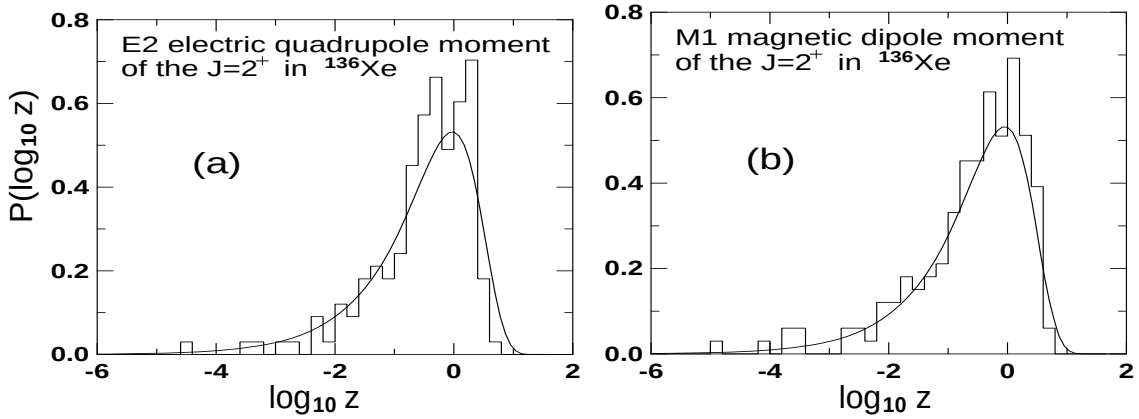

Fig.5. The statistics of (a) the $E2$ ***electric quadrupole moments and (b) the*** $M1$ ***magnetic dipole moments of the*** $J = 2^+$ ***states in*** ^{136}Xe ***nucleus. The histograms show the distribution*** $P(\log_{10} z)$, ***where*** z ***are squares of*** $E2$ ***or*** $M1$ ***diagonal reduced matrix elements whose mean value [eq. (12)] has been subtracted. The solid lines describe Porter-Thomas distribution.***